Available online at www.sciencedirect.com
SCIENCE DIRECT®
ELSEVIER
International Journal of Solids and Structures 42 (2005) 5243–5258
INTERNATIONAL JOURNAL OF SOLIDS and STRUCTURES
www.elsevier.com/locate/ijsolstr

A comprehensive analysis of functionally graded sandwich plates: Part 2—Buckling and free vibration

A.M. Zenkour *

Department of Mathematics, Faculty of Education, Tanta University, Kafr El-Sheikh 33516, Egypt

Received 12 June 2004; received in revised form 10 February 2005
Available online 14 April 2005

Abstract

The sinusoidal shear deformation plate theory, presented in the first part of this paper, is used to study the buckling and free vibration of the simply supported functionally graded sandwich plate. Effects of rotatory inertia are considered. The critical buckling load and the vibration natural frequency are investigated. Some available results for sandwich plates non-symmetric about the mid-plane can be retrieved from the present analysis. The influences of the transverse shear deformation, plate aspect ratio, side-to-thickness ratio and volume fraction distributions are studied. In addition, the effect of the core thickness, relative to the total thickness of the plate, on the critical buckling load and the eigenfrequencies is investigated.

Keywords: Functionally graded material; Sandwich plate; Critical buckling load; Natural frequencies; Sinusoidal theory

1. Introduction

In Part 1 of this paper (Zenkour, 2005a) a sinusoidal shear deformation theory of functionally graded sandwich plates was presented. Starting with this theory and other theories, the state of deflection and stresses of sandwich plates was analyzed. In this part the free vibration and buckling problems of such plates are studied.

Here we present a sandwich plate; its faces are typically made from a mixture of ceramic and metal materials with a desired variation of the volume fractions of the two materials in between the two

* Tel.: +20 473238907; fax: +20 473223415.
E-mail address: zenkour@powernet.com.eg.

0020-7683/$ - see front matter © 2005 Elsevier Ltd. All rights reserved.
doi:10.1016/j.ijsolstr.2005.02.016

surfaces of each face. The core material of the present sandwich plate is fully ceramic. The composition of the bottom face is varied from a metal-rich surface to a ceramic-rich surface while that of the top face is varied from a ceramic-rich surface to a metal-rich surface. The ceramic constituent of the material provides the high-temperature resistance due to its low thermal conductivity (Hasselman and Youngblood, 1978). The gradual change of material properties can be tailored to different applications and high temperature working environments (Hasselman and Youngblood, 1978; Yamanouchi et al., 1990; Fukui and Yamanaka, 1992; Koizumi, 1993). This makes functionally graded materials (FGMs) preferable in many applications. A listing of different applications can be found in the literature (FGM Forum, 1991).

Several studies have been performed to analyze the behaviour of FG structures (Praveen and Reddy, 1998; Reddy and Chin, 1998; Reddy, 2000; Cheng and Batra, 2000a,b; Vel and Batra, 2002). The response of FG ceramic–metal plates has been investigated by Praveen and Reddy (1998) using a plate finite element that accounts for the transverse shear strains, rotatory inertia and moderately large rotations in von Kármán sense. Reddy and Chin (1998) have studied the dynamic thermoelastic response of FG cylinders and plates. Reddy (2000) has presented solutions for FG rectangular plates based on his third-order shear deformation plate theory. Cheng and Batra (2000a) have related the deflections of a simply supported FG polygonal plate given by the first-order shear deformation theory and a third-order shear deformation theory to that of an equivalent homogeneous Kirchhoff plate. Cheng and Batra (2000b) have used the method of asymptotic expansion to study the 3D thermoelastic deformations of FG elliptic plates. Recently, Vel and Batra (2002) have presented an exact 3D solution for the thermoelastic deformation of FG simply supported plates of finite dimensions.

Among numerous studies on FGMs, an interesting issue is the correspondence between the buckling load and vibration frequencies of plates and shells. However, the analysis of buckling and vibration of FGM structures are rare in the literature. Birman (1995) studied the buckling problem of FG composite rectangular plate subjected to the uniaxial compression. Loy et al. (1999) have studied the vibration of FG cylindrical shells using Love's shell theory. Cheng and Batra (2000c) have also presented results for the buckling and steady state vibrations of a simply supported FG polygonal plate based on Reddy's plate theory (Reddy, 2000). The stabilization of FG cylindrical shells under axial harmonic loading is investigated by Ng et al. (2001). Javaheri and Eslami (2002a,b,c) presented thermal and mechanical buckling of rectangular FGM plates based on the first- and higher-order plate theories. The thermal buckling load of, and the buckling analysis of radially loaded solid, circular FGM plates are given by Najafizadeh and Eslami (2002a,b).

From a technical point of view, results of critical buckling load and vibration frequencies enable one to bypass more complicated calculations for plate theories. Such correspondences have been established between frequencies of single-layer homogeneous, sandwich, and laminated plates analyzed by using different plate theories. However, these results are valid only for plates that are materially and geometrically symmetric or non-symmetric about the mid-plane. Here we present FG sandwich plate with material properties symmetric about the mid-plane (see Fig. 1). The faces of the plate consist of a FGM with properties varying only in the thickness direction. Such faces can be made by mixing two different material phases, for example, a metal and a ceramic. The core material may be homogeneous and can be made by one of these materials, for example, a ceramic. Eigenfrequencies and critical buckling loads of FG sandwich plates are presented using the sinusoidal shear deformation theory (Zenkour, 2004a,b,c, 2005b). It is clear from now that the results of the ceramic plates are much higher than those of the metallic plates. The results of the graded plates are intermediate to those of the ceramic and metal plates. Thus, the gradients in material properties play an important role in determining the critical buckling loads and the free vibration frequencies of the FGM sandwich plates. Results for the classical, first- and third-order plate theories can also be obtained from the present analysis. Comparisons with the existing literature are made.

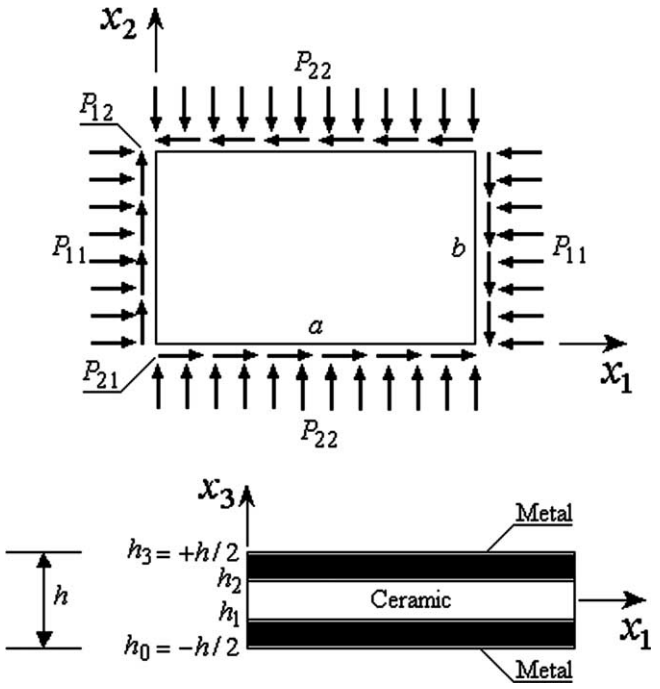

Fig. 1. Geometry of the FGM sandwich rectangular plate.

2. Governing equations

Let the upper surface of the plate ($x_3 = h/2$) be subjected to a transverse distributed load $q(x, y)$. There be distributed compressive in-plane forces P_{11} and P_{22}, and a distributed shear force P_{12} (per unit length) acting on the mid-plane of the plate (see Fig. 1). The dynamic version of the principle of virtual displacements in the present case yields

$$\int_{-h/2}^{h/2}\int_{\Omega}\left[\rho^{(n)}\ddot{v}_i\delta v_i + \sigma_{11}^{(n)}\delta e_{11} + \sigma_{22}^{(n)}\delta e_{22} + \cdots\right]\mathrm{d}\Omega\,\mathrm{d}x_3 - \int_{\Omega}\left[q\delta u_3 + P_{\alpha\beta}u_{3,\beta}\delta u_{3,\alpha}\right]\mathrm{d}\Omega = 0, \tag{1}$$

or

$$\int_{\Omega}\left[\int_{-h/2}^{h/2}\rho^{(n)}\ddot{v}_i\delta v_i\,\mathrm{d}x_3 + N_{\alpha\beta}\delta\varepsilon_{\alpha\beta} + M_{\alpha\beta}\delta\kappa_{\alpha\beta} + S_{\alpha\beta}\delta\eta_{\alpha\beta} + Q_{\alpha 3}\delta\varepsilon_{\alpha 3} - q\delta u_3 - P_{\alpha\beta}u_{3,\beta}\delta u_{3,\alpha}\right]\mathrm{d}\Omega = 0, \tag{2}$$

where $\rho^{(n)}$ is the material density of the nth layer; $N_{\alpha\beta}$ and $M_{\alpha\beta}$ are the basic components of stress resultants and stress couples; $S_{\alpha\beta}$ are additional stress couples associated with the transverse shear effects; and $Q_{\alpha 3}$ are transverse shear stress resultants.

The governing equations of motion can be derived from Eq. (2) by integrating the displacement gradients in e_{ij} by parts and setting the coefficients δu_i and $\delta\varphi_\alpha$ to zero separately. Thus one can obtain

$$\begin{aligned}
&N_{\alpha\beta,\beta} - I^{11}\ddot{u}_\alpha + I^{12}\ddot{u}_{3,\alpha} - I^{13}\ddot{\varphi}_\alpha = 0,\\
&M_{\alpha\beta,\alpha\beta} - I^{11}\ddot{u}_3 - I^{12}\ddot{u}_{\alpha,\alpha} + I^{22}\ddot{u}_{3,\alpha\alpha} - I^{23}\ddot{\varphi}_{\alpha,\alpha} - \left(P_{\alpha\beta}u_{3,\beta}\right)_{,\alpha} + q = 0,\\
&S_{\alpha\beta,\beta} - Q_{\alpha 3} - I^{13}\ddot{u}_\alpha + I^{23}\ddot{u}_{3,\alpha} - I^{33}\ddot{\varphi}_\alpha = 0,
\end{aligned} \tag{3}$$

where

$$[I] = \begin{bmatrix} I^{11} & I^{12} & I^{13} \\ I^{12} & I^{22} & I^{23} \\ I^{13} & I^{23} & I^{33} \end{bmatrix} = \sum_{n=1}^{3} \int_{h_{n-1}}^{h_n} \rho^{(n)} \begin{bmatrix} 1 & x_3 & \Psi \\ x_3 & x_3^2 & x_3\Psi \\ \Psi & x_3\Psi & \Psi^2 \end{bmatrix} \mathrm{d}x_3. \tag{4}$$

With the help of stress resultants, Eq. (3) gives the following equations for all theories.

SSDPT and TSDPT:

$$A^{11}u_{1,11} + \frac{1}{2}B^{11}u_{1,22} + \left(A^{11} - \frac{1}{2}B^{11}\right)u_{2,12} - A^{12}\nabla^2 u_{3,1} + A^{13}\varphi_{1,11} + \frac{1}{2}B^{13}\varphi_{1,22} + \left(A^{13} - \frac{1}{2}B^{13}\right)\varphi_{2,12} - I^{11}\ddot{u}_1 + I^{12}\ddot{u}_{3,1} - I^{13}\ddot{\varphi}_1 = 0, \quad (1 \leftrightarrow 2), \tag{5a}$$

$$A^{12}(\nabla^2 u_{1,1} + \nabla^2 u_{2,2}) - A^{22}\nabla^4 u_3 + A^{23}(\nabla^2\varphi_{1,1} + \nabla^2\varphi_{2,2}) + q - I^{11}\ddot{u}_3 - I^{12}(\ddot{u}_{1,1} + \ddot{u}_{2,2}) + I^{22}\nabla^2\ddot{u}_3 - I^{23}(\ddot{\varphi}_{1,1} + \ddot{\varphi}_{2,2}) - (P_{11}u_{3,1} + P_{12}u_{3,2})_{,1} - (P_{12}u_{3,1} + P_{22}u_{3,2})_{,2} = 0, \tag{5b}$$

$$A^{13}u_{1,11} + \frac{1}{2}B^{13}u_{1,22} + \left(A^{13} - \frac{1}{2}B^{13}\right)u_{2,12} - A^{23}\nabla^2 u_{3,1} + A^{33}\varphi_{1,11} + \frac{1}{2}B^{33}\varphi_{1,22} + \left(A^{33} - \frac{1}{2}B^{33}\right)\varphi_{2,12} - C\varphi_1 - I^{13}\ddot{u}_1 + I^{23}\ddot{u}_{3,1} - I^{33}\ddot{\varphi}_1 = 0, \quad (1 \leftrightarrow 2), \tag{5c}$$

where the sign $(1 \leftrightarrow 2)$ indicates that from Eqs. (5a) and (5c) other equations may be obtained by interchanging the sub-index 1 by 2 and vice-versa and $\nabla^2(\,) = (\,)_{,11} + (\,)_{,22}$ is *Laplace* operator.

FSDPT:

$$A^{11}(u_{1,1} + u_{2,2})_{,1} + \frac{1}{2}B^{11}(u_{1,2} - u_{2,1})_{,2} + A^{12}(\varphi_{1,1} + \varphi_{2,2} - \nabla^2 u_3)_{,1} + \frac{1}{2}B^{12}(\varphi_{1,2} - \varphi_{2,1})_{,2} - I^{11}\ddot{u}_1 - I^{12}(\ddot{\varphi}_1 - \ddot{u}_{3,1}) = 0, \quad (1 \leftrightarrow 2), \tag{6a}$$

$$A^{12}(\nabla^2 u_{1,1} + \nabla^2 u_{2,2}) + A^{22}(\nabla^2\varphi_{1,1} + \nabla^2\varphi_{2,2} - \nabla^4 u_3) + q - I^{11}\ddot{u}_3 - I^{12}(\ddot{u}_{1,1} + \ddot{u}_{2,2}) - I^{22}(\ddot{\varphi}_{1,1} + \ddot{\varphi}_{2,2} - \nabla^2\ddot{u}_3) - (P_{11}u_{3,1} + P_{12}u_{3,2})_{,1} - (P_{12}u_{3,1} + P_{22}u_{3,2})_{,2} = 0, \tag{6b}$$

$$A^{12}(u_{1,1} + u_{2,2})_{,1} + \frac{1}{2}B^{12}(u_{1,2} - u_{2,1})_{,2} + A^{22}(\varphi_{1,1} + \varphi_{2,2} - \nabla^2 u_3)_{,1} + \frac{1}{2}B^{22}(\varphi_{1,2} - \varphi_{2,1})_{,2} - C_F\varphi_1 - I^{12}\ddot{u}_1 - I^{22}(\ddot{\varphi}_1 - \ddot{u}_{3,1}) = 0, \quad (1 \leftrightarrow 2), \tag{6c}$$

where

$$C_F = \sum_{n=1}^{3} \int_{h_{n-1}}^{h_n} KG'_{(n)}\,\mathrm{d}x_3, \tag{7}$$

in which K is the shear correction factor.

CLPT:

$$A^{11}(u_{1,1}+u_{2,2})_{,1}+\frac{1}{2}B^{11}(u_{1,2}-u_{2,1})_{,2}-A^{12}\nabla^2 u_{3,1}-I^{11}\ddot{u}_1+I^{12}\ddot{u}_{3,1}=0,\quad (1\leftrightarrow 2), \tag{8a}$$

$$A^{12}(\nabla^2 u_{1,1}+\nabla^2 u_{2,2})-A^{22}\nabla^4 u_3+q-I^{11}\ddot{u}_3-I^{12}(\ddot{u}_{1,1}+\ddot{u}_{2,2})+I^{22}\nabla^2\ddot{u}_3-(P_{11}u_{3,1}+P_{12}u_{3,2})_{,1}$$
$$-(P_{12}u_{3,1}+P_{22}u_{3,2})_{,2}=0. \tag{8b}$$

3. Exact solutions for FGMs sandwich plates

Rectangular plates are generally classified in accordance with the type support used. We are here concerned with the exact solutions of Eqs. (5), (6) and (8) for simply supported FGM plate.

3.1. The free vibration problem of sandwich plates

The following representation for the displacement quantities of the shear deformation theories is appropriate in the case of the free vibration problem ($P_{11}=P_{12}=P_{22}=q=0$):

$$\begin{Bmatrix} u_1\\ u_2\\ u_3\\ \varphi_1\\ \varphi_2 \end{Bmatrix}=\begin{Bmatrix} U_1\cos(\lambda x)\sin(\mu y)\\ U_2\sin(\lambda x)\cos(\mu y)\\ U_3\sin(\lambda x)\sin(\mu y)\\ \Phi_1\cos(\lambda x)\sin(\mu y)\\ \Phi_2\sin(\lambda x)\cos(\mu y) \end{Bmatrix}e^{i\omega t}. \tag{9}$$

Here $\lambda=r\pi/a$, $\mu=s\pi/b$, and U_1, U_2, U_3, Φ_1 and Φ_2 being arbitrary parameters and $\omega=\omega_{rs}$ denotes the eigenfrequency associated with (rth, sth) eigenmode. Eq. (9) is appropriate for CLPT by ignoring the functions φ_1 and φ_2.

Eqs. (5), (6) and (8) in conjunction with Eq. (9) can be combined into a system of first-order equations as:

$$([L]-\omega^2[R])\{\Delta\}=\{0\}, \tag{10}$$

where the matrices $\{\Delta\}$ and $[L]$ are given according to all theories in the first part of this paper (Zenkour, 2005a) while the elements of matrix $[R]$ are defined in Appendix A. The condition expresses by $\det([L]-\omega^2[R])=0$ yields the eigenfrequencies ω.

For the sake of completeness and comparison, the analytical solution for the vibration problem of thin, isotropic, rectangular plates is presented here as given in most literature (see, e.g., Leissa, 1973),

$$\omega=\frac{\pi^2}{a^2}\sqrt{\frac{D}{\rho h}}\left[r^2+\left(\frac{a}{b}\right)^2 s^2\right], \tag{11}$$

where ρ is the material density, r and s are the mode numbers and

$$D=\frac{Eh^3}{12(1-\nu^2)} \tag{12}$$

is the flexural rigidity of the plate with E and ν as Young's modulus and Poisson's ratio.

3.2. The static buckling problem of sandwich plates

The representation in Eq. (9) specialized for $\omega \to 0$ is appropriate in dealing with the static compressive buckling problem. The obtained equations allow one to derive some results which concern the buckling of FG sandwich plates subjected to a system of uniform in-plane compressive loads P_{11} and P_{22} ($P_{12} = 0$). Assuming that there is a given ratio between these forces such that $P_{11} = -P$ and $P_{22} = -\gamma P$; $\gamma = P_{22}/P_{11}$, we get

$$([L] - P[H])\{\Delta\} = \{0\}. \tag{13}$$

The elements of the matrix $[H]$ are zeros except $H^{33} = \lambda^2 + \gamma\mu^2$. The condition expressed by $\det([L] - P[H]) = 0$ yields the buckling loads.

4. Numerical results

To verify the analytical formulation presented in the previous sections, six different types of FG plates are considered. Sandwich plates that are symmetric and non-symmetric about their middle plane are examined. Note that the core of the plate is fully ceramic while the bottom and top surfaces of the plate are metal-rich.

In the first part of this paper (Zenkour, 2005a), five types of FG sandwich plate are presented. Here an additional case of (2-1-1) FGM sandwich plate is investigated. The top face thickness is the same as the core thickness while the bottom face thickness is twice the core thickness. So in this case we have $h_1 = 0$ and $h_2 = h/4$.

For the sake of clarity, Fig. 2 shows the through-the-thickness variation of the volume fraction function of the ceramic for $k = 0.02, 0.2, 1, 2, 5$. Two different types, (2-1-2) and (2-1-1) FGM sandwich plates, are considered.

The FG plate is taken to be made of aluminum and alumina with the following material properties:

$$E_m = 70E_0, \qquad \rho_m = 2707\rho_0 \quad \text{for aluminum},$$

$$E_c = 380E_0, \qquad \rho_c = 3800\rho_0 \quad \text{for alumina},$$

where the reference values are taken as $E_0 = 1$ GPa and $\rho_0 = 1$ kg/m^3.

For simplicity, Poisson's ratio is chosen as $\nu_m = \nu_c = \nu = 0.3$ for both aluminum and alumina. We also take the shear correction factor $K = 5/6$ in FSDPT.

Numerical results are presented in terms of natural vibration frequencies and critical buckling loads. The various non-dimensional parameters used are:

$$\text{thickness coordinate } \bar{x}_3\text{:} \quad \frac{x_3}{h},$$

$$\text{natural frequency } \bar{\omega}\text{:} \quad \frac{\omega a^2}{h}\sqrt{\frac{\rho_0}{E_0}},$$

$$\text{critical buckling load } \overline{P}\text{:} \quad \frac{Pa^2}{100h^3E_0}.$$

Numerical results are tabulated in Tables 1–8 and plotted in Figs. 3–6. It is assumed (unless otherwise stated) that $a/h = 10$ and $a/b = 1$. Tables 1–3 display the critical buckling loads and eigenfrequencies obtained in the framework of various plate theories. The results obtained in Reddy (1984), as per the

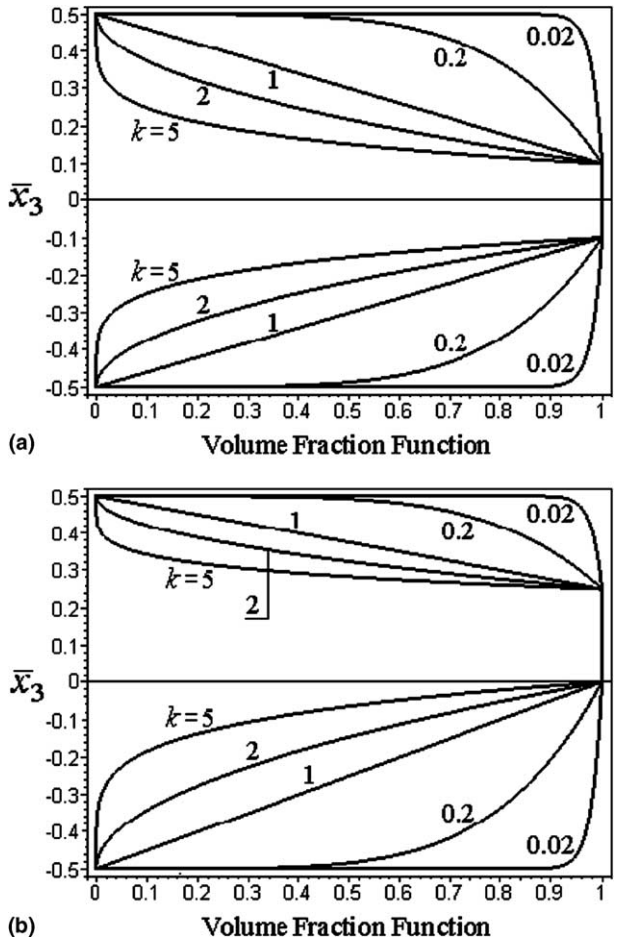

Fig. 2. Variation of volume fraction function through plate thickness for various values of the power-law index k of symmetric and non-symmetric sandwich plates. (a) The (2-1-2) FGM sandwich plate and (b) the (2-1-1) FGM sandwich plate.

higher-order shear deformation theory (HSDT), and of the theory referred as DT developed in Librescu et al. (1990) are used in the comparisons. An accurate three-dimensional elasticity solution by the differential quadrature method (DQM) of Malik and Bert (1998) for free vibrations of isotropic plates is also used to assess the improvement in the prediction of frequencies.

First, Table 1 provides some sample results showing the accuracy of the present critical loads. The material of the plate is considered as a fully transversely-isotropic with the following properties:

$$E = 20.83 \times 10^6 \text{ psi } (145.81 \text{ GPa}), \quad E' = 10^7 \text{ psi } (70 \text{ GPa}),$$

$$G' = 3.71 \times 10^6 \text{ psi } (25.97 \text{ GPa}), \quad v = v' = 0.44.$$

It is apparent that the critical buckling loads obtained by the TSDPT are the same as those of Reddy (1984) using HSDT. This is not surprise because the two theories are the same. In addition, the results of FSDPT are identical to those given in Librescu et al. (1990) using DT.

Table 1
Buckling loads $P^* = Pa^2/(h^3E)$ of a fully transversely-isotropic square plate ($r = s = 1$)

γ	Theory	a/h				
		2	5	10	20	50
0.0	HSDT (Reddy, 1984)	0.9486	2.6386	3.5875	3.9442	4.0574
	DT (Librescu et al., 1990)	0.9197	2.6325	3.5868	3.9442	4.0574
	SSDPT	0.95624	2.64134	3.58825	3.94444	4.05743
	TSDPT	0.94858	2.63860	3.58746	3.94423	4.05739
	FSDPT	0.91971	2.63251	3.58676	3.94418	4.05739
0.5	HSDT (Reddy, 1984)	0.6324	1.7591	2.3916	2.6295	2.7049
	DT (Librescu et al., 1990)	0.6131	1.7550	2.3912	2.6295	2.7049
	SSDPT	0.63749	1.76090	2.39168	2.62962	2.70495
	TSDPT	0.63239	1.75906	2.39164	2.62949	2.70493
	FSDPT	0.61314	1.75501	2.39117	2.62945	2.70493
1.0	HSDT (Reddy, 1984)	0.4743	1.3193	1.7937	1.9721	2.0287
	DT (Librescu et al., 1990)	0.4599	1.3163	1.7934	1.9721	2.0287
	SSDPT	0.47812	1.32067	1.79413	1.97222	2.02871
	TSDPT	0.47429	1.31930	1.79373	1.97212	2.02870
	FSDPT	0.45985	1.31626	1.79338	1.97209	2.02870

$\text{CLPT}_{|\gamma=0} = 4.07970$, $\text{CLPT}_{|\gamma=0.5} = 2.71980$ and $\text{CLPT}_{|\gamma=1} = 2.03985$.

Table 2
Fundamental frequencies $\omega^* = (\omega a^2/2\pi)\sqrt{\rho h/D}$ of an isotropic rectangular plate ($b = 2a$, Analytical solution (Leissa, 1973) is 1.963495)

h/b	CLPT	FSDPT	TSDPT	SSDPT	DQM solution (Malik and Bert, 1998)
0.2	1.81954	1.51101	1.51230	1.51294	1.53118
0.1	1.92433	1.80958	1.80974	1.80993	1.81513
0.02	1.96188	1.95639	1.95639	1.95640	1.95667
0.01	1.96309	1.96171	1.96171	1.96171	1.96179
0.005	1.96339	1.96305	1.96305	1.96305	1.96299

Table 3
Natural frequencies $\omega^* = (\omega a^2/2\pi)\sqrt{\rho h/D}$ of an isotropic square plate

h/b	r	s	CLPT	FSDPT	TSDPT	TSDPT	DQM solution (Malik and Bert, 1998)
0.2	1	1	3.04307	2.77612	2.77669	2.77717	2.78935
	1	2	7.27816	6.04406	6.04919	6.05177	6.12471
	2	2	11.18087	8.65997	8.67383	8.67960	8.87880
	1	3	13.62572	10.155636	10.17716	10.18547	10.5036
0.1	1	1	3.11607	3.03428	3.03433	3.03445	3.03828
	1	2	7.69731	7.23830	7.23897	7.23973	7.26053
	2	2	12.17230	11.10448	11.10688	11.10867	11.1574
	1	3	15.09930	13.52525	13.52929	13.53217	13.6058
	2	3	19.40908	16.96226	16.96226	16.96698	17.0884
	1	4	25.01214	21.20180	21.21607	21.22378	21.4318

Table 4
Effects of volume fraction exponent on the fundamental frequencies of an FGM square plate

k	Theory	$\bar{\omega}$					
		1-0-1	2-1-2	2-1-1	1-1-1	2-2-1	1-2-1
0	CLPT	1.87359	1.87359	1.87359	1.87359	1.87359	1.87359
	FSDPT	1.82442	1.82442	1.82442	1.82442	1.82442	1.82442
	TSDPT	1.82445	1.82445	1.82445	1.82445	1.82445	1.82445
	SSDPT	1.82452	1.82452	1.82452	1.82452	1.82452	1.82452
0.5	CLPT	1.47157	1.51242	1.54264	1.54903	1.58374	1.60722
	FSDPT	1.44168	1.48159	1.51035	1.51695	1.55001	1.57274
	TSDPT	1.44424	1.48408	1.51253	1.51922	1.55199	1.57451
	SSDPT	1.44436	1.48418	1.51258	1.51927	1.55202	1.57450
1	CLPT	1.26238	1.32023	1.37150	1.37521	1.43247	1.46497
	FSDPT	1.24031	1.29729	1.34637	1.35072	1.40555	1.43722
	TSDPT	1.24320	1.30011	1.34888	1.35333	1.40789	1.43934
	SSDPT	1.24335	1.30023	1.34894	1.35339	1.40792	1.43931
5	CLPT	0.95844	0.99190	1.08797	1.05565	1.16195	1.18867
	FSDPT	0.94256	0.97870	1.07156	1.04183	1.14467	1.17159
	TSDPT	0.94598	0.98184	1.07432	1.04466	1.14731	1.17397
	SSDPT	0.94630	0.98207	1.07445	1.04481	1.14741	1.17399
10	CLPT	0.94321	0.95244	1.05185	1.00524	1.11883	1.13614
	FSDPT	0.92508	0.93962	1.03580	0.99256	1.10261	1.12067
	TSDPT	0.92839	0.94297	1.03862	0.99551	1.10533	1.12314
	SSDPT	0.92875	0.94332	1.04558	0.99519	1.04154	1.13460

Table 5
Effects of volume fraction exponent on the uniaxial buckling load of an FGM square plate ($\gamma = 0$)

k	Theory	$\overline{P}$					
		1-0-1	2-1-2	2-1-1	1-1-1	2-2-1	1-2-1
0	CLPT	13.73791	13.73791	13.73791	13.73791	13.73791	13.73791
	FSDPT	13.00449	13.00449	13.00449	13.00449	13.00449	13.00449
	TSDPT	13.00495	13.00495	13.00495	13.00495	13.00495	13.00495
	SSDPT	13.00606	13.00606	13.00606	13.00606	13.00606	13.00606
0.5	CLPT	7.65398	8.25597	8.56223	8.78063	9.18254	9.61525
	FSDPT	7.33732	7.91320	8.20015	8.41034	8.78673	9.19517
	TSDPT	7.36437	7.94084	8.22470	8.43645	8.80997	9.21681
	SSDPT	7.36568	7.94195	8.22538	8.43712	8.81037	9.21670
1	CLPT	5.33248	6.02733	6.40391	6.68150	7.19663	7.78406
	FSDPT	5.14236	5.81379	6.17020	6.43892	6.92571	7.48365
	TSDPT	5.16713	5.84006	6.19394	6.46474	6.94944	7.50656
	SSDPT	5.16846	5.84119	6.19461	6.46539	6.94980	7.50629
5	CLPT	2.73080	3.10704	3.48418	3.65732	4.21238	4.85717
	FSDPT	2.63842	3.02252	3.38538	3.55958	4.09285	4.71475
	TSDPT	2.65821	3.04257	3.40351	3.57956	4.11209	4.73469
	SSDPT	2.66006	3.04406	3.40449	3.58063	4.11288	4.73488
10	CLPT	2.56985	2.80340	3.16427	3.25924	3.79238	4.38221
	FSDPT	2.46904	2.72626	3.07428	3.17521	3.68890	4.26040
	TSDPT	2.48727	2.74632	3.09190	3.19471	3.70752	4.27991
	SSDPT	2.48928	2.74844	3.13443	3.19456	3.14574	4.38175

Table 6
Effects of volume fraction exponent on the biaxial buckling load of an FGM square plate ($\gamma = 1$)

k	Theory	$\overline{P}$					
		1-0-1	2-1-2	2-1-1	1-1-1	2-2-1	1-2-1
0	CLPT	6.86896	6.86896	6.86896	6.86896	6.86896	6.86896
	FSDPT	6.50224	6.50224	6.50224	6.50224	6.50224	6.50224
	TSDPT	6.50248	6.50248	6.50248	6.50248	6.50248	6.50248
	SSDPT	6.50303	6.50303	6.50303	6.50303	6.50303	6.50303
0.5	CLPT	3.82699	4.12798	4.28112	4.39032	4.59127	4.80762
	FSDPT	3.66866	3.95660	4.10007	4.20517	4.39336	4.59758
	TSDPT	3.68219	3.97042	4.11235	4.21823	4.40499	4.60841
	SSDPT	3.68284	3.97097	4.11269	4.21856	4.40519	4.60835
1	CLPT	2.66624	3.01366	3.20195	3.34075	3.59831	3.89203
	FSDPT	2.57118	2.90690	3.08510	3.21946	3.46286	3.74182
	TSDPT	2.58357	2.92003	3.09697	3.23237	3.47472	3.75328
	SSDPT	2.58423	2.92060	3.09731	3.23270	3.47490	3.75314
5	CLPT	1.36540	1.55352	1.74209	1.82866	2.10619	2.42859
	FSDPT	1.31921	1.51126	1.69269	1.77979	2.04642	2.35737
	TSDPT	1.32910	1.52129	1.70176	1.78978	2.05605	2.36734
	SSDPT	1.33003	1.52203	1.70224	1.79032	2.05644	2.36744
10	CLPT	1.28493	1.40170	1.58214	1.62962	1.89619	2.19111
	FSDPT	1.23452	1.36313	1.53714	1.58760	1.84445	2.13020
	TSDPT	1.24363	1.37316	1.54595	1.59736	1.85376	2.13995
	SSDPT	1.24475	1.37422	1.56721	1.59728	1.57287	2.19087

Table 7
Natural frequencies $\bar{\omega}$ of an FGM square plate ($k = 2$)

r	s	1-2-1				2-2-1			
		CLPT	FSDPT	TSDPT	SSDPT	CLPT	FSDPT	TSDPT	SSDPT
1	1	1.32200	1.30020	1.30246	1.30244	1.28650	1.26524	1.26775	1.26780
1	2	3.26976	3.14452	3.15698	3.15686	3.18172	3.05968	3.07353	3.07382
2	2	5.17700	4.88021	4.90879	4.90849	5.03724	4.74815	4.77998	4.78065
1	3	6.42690	5.98487	6.02667	6.02622	6.25311	5.82264	5.86924	5.87022
2	3	8.27066	7.57215	7.63674	7.63601	8.04649	7.36640	7.43850	7.44002
1	4	10.67355	9.57284	9.67233	9.67121	10.38339	9.31198	9.42315	9.42552
3	3	11.26475	10.05424	10.16314	10.16193	10.95830	9.78007	9.90179	9.90439
2	4	12.43611	10.99612	11.12461	11.12321	12.09731	10.69588	10.83951	10.84261
3	4	15.30248	13.23801	13.41936	13.41755	14.88418	12.87543	13.07809	13.08260
4	4	19.17579	16.13722	16.40035	16.39820	18.64932	15.69346	15.98701	15.99393

Table 2 shows some sample results of the fundamental frequencies of isotropic rectangular plates for decreasing values of the thickness ratio (h/b). The results of the present sinusoidal shear deformation theory compared well with the DQM solution (Malik and Bert, 1998). As one would expect, it may be seen that with plates becoming thinner, the fundamental frequencies in all cases approach to values of the analytical thin plate solution (Leissa, 1973).

Next, we have displayed the natural frequencies of an isotropic square plate according to various theories and DQM solution in Table 3. It may be seen that there is a close agreement between the present

Table 8
Effect of the aspect ratio on the critical buckling load $\overline{P}$ of an FGM rectangular plate ($k = 2$)

γ	b/a	1-2-1				2-2-1			
		CLPT	FSDPT	TSDPT	SSDPT	CLPT	FSDPT	TSDPT	SSDPT
0.0	0.5[a]	14.69209	23.86154	23.94786	23.94721	12.01416	21.29983	21.38582	21.38784
	1.0	5.96539	5.96539	5.98697	5.98680	5.50354	5.32496	5.32496	5.34696
	2.0	2.41134	2.21831	2.23758	2.23745	2.14982	1.98352	2.00278	2.00325
0.5	0.5	12.86046	12.58665	12.61540	12.61518	11.46571	11.23031	11.25893	11.25960
	1.0	4.11535	3.97692	3.99131	3.99120	3.66903	3.54997	3.56430	3.56464
	2.0	2.14341	1.97183	1.98896	1.98885	1.91095	1.76313	1.78025	1.78067
1.0	0.5	7.71628	7.55199	7.56924	7.56911	6.87943	6.73819	6.75536	6.75576
	1.0	3.08651	2.98269	2.99348	2.99340	2.75177	2.66248	2.67323	2.67348
	2.0	1.92907	1.77464	1.79006	1.78996	1.71986	1.58681	1.60222	1.60260

[a] Critical buckling occurs at (2,1).

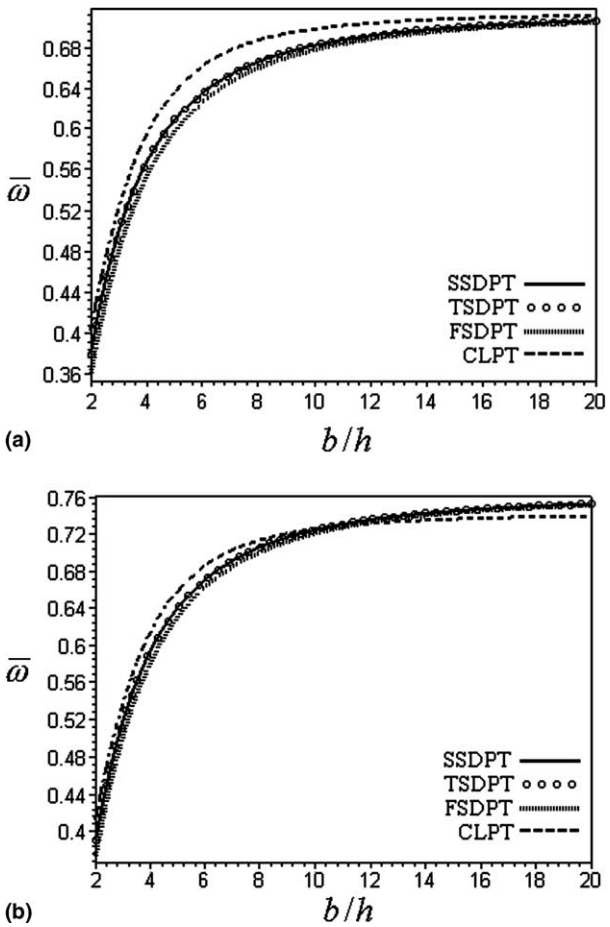

Fig. 3. Fundamental frequency ($\bar{\omega}$) as a function of side-to-thickness ratio (b/h) of symmetric and non-symmetric FGM sandwich plates using various plate theories ($b = 2a$, $k = 2$). (a) The (2-1-2) FGM sandwich plate and (b) the (2-1-1) FGM sandwich plate.

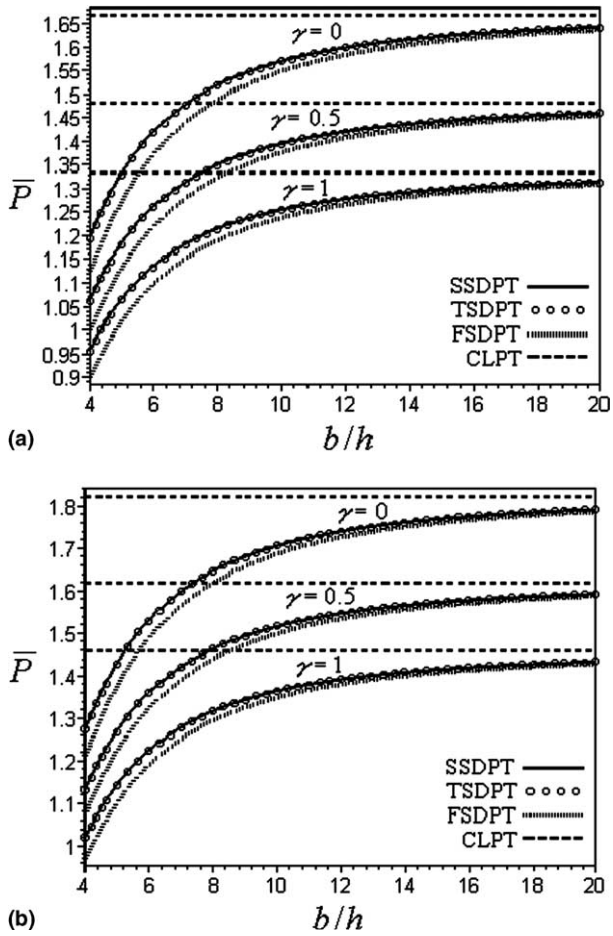

Fig. 4. Buckling load ($\overline{P}$) as a function of side-to-thickness ratio (b/h) of symmetric and non-symmetric FGM sandwich plates using various plate theories ($b = 2a$, $k = 2$). (a) The (2-1-2) FGM sandwich plate and (b) the (2-1-1) FGM sandwich plate.

sinusoidal shear deformation solution and the DQM solution. In fact, the SSDPT gives buckling loads (see Table 1) and vibration frequencies (see Tables 2 and 3) higher that other shear deformation theories. However, the SSDPT frequencies are slightly lower than the elasticity DQM solution values.

Tables 4–6 provide fundamental frequencies and critical buckling loads of six types of FG sandwich plates using various plate theories and different values of the volume fraction exponent k. Of these results, the frequencies and critical buckling loads decrease as k increases and as the core thickness, with respect to the total thickness of the plate, decreases. An exception of this occurs when $k \geqslant 5$ in which the frequencies of an (1-1-1) FG plate are more than the ones of an (2-1-1) FG plate. The (1-2-1) FG plate case shows the highest sensitivity in the context of the considered FG sandwich plate types. In general, the fully ceramic plates give the largest frequencies and critical buckling loads. The uniaxial buckling load may be twice the biaxial one and this irrespective of the considered value of k and the type of the FG plate.

Comparisons are given in Tables 7 and 8 on the basis of the symmetric (1-2-1) and non-symmetric (2-2-1) types of FG sandwich plates. The frequencies increase as the mode number increases while the critical buckling loads decrease with increasing aspect ratio (b/a) and γ. In general, the vibration frequencies and the

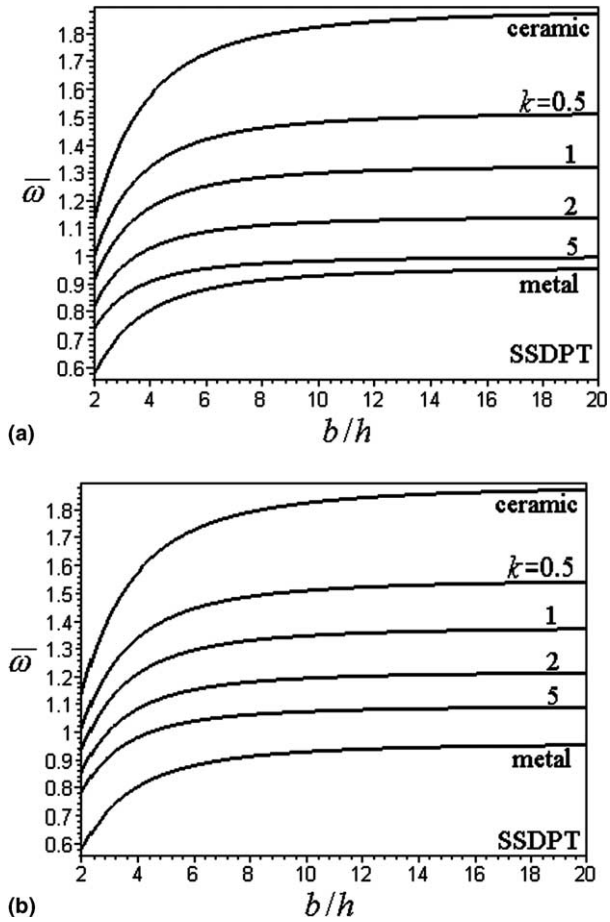

Fig. 5. Fundamental frequency ($\bar{\omega}$) as a function of side-to-thickness ratio (b/h) of symmetric and non-symmetric FGM sandwich plates for various values of k. (a) The (2-1-2) FGM sandwich plate and (b) the (2-1-1) FGM sandwich plate.

critical buckling loads obtained by the CLPT are much higher than those computed from the shear deformation theories. This implies the well-known fact that the results estimated by the CLPT are grossly in error for a thick plate and/or for higher mode numbers.

Figs. 3 and 4 exhibit plots of the fundamental frequencies and critical buckling loads versus the side-to-thickness ratio for $k = 2$ and $b = 2a$. As expected, errors in the solutions obtained from the FSDPT and the CLPT increase as the side-to-thickness ratio decreases. Among the four plate theories considered here, the CLPT gives the highest frequency for the (2-1-2) FG sandwich plate while its behaviour is changed from the highest to the lowest frequency when $b/h \cong 11$ for the (2-1-1) FG plate (see Fig. 3). Fig. 4 shows, once again the well-known fact, that the critical buckling loads of the CLPT are independent of the b/h ratio. The critical buckling loads decrease as γ increases. The results of the non-symmetric plate are higher than the corresponding ones for the symmetric plate and this depend on the thickness of the core layer.

Figs. 5 and 6 depict the vibration frequencies and the critical buckling loads versus the side-to-thickness ratio using TSDPT. The results are the maximum for the ceramic plates and the minimum for the

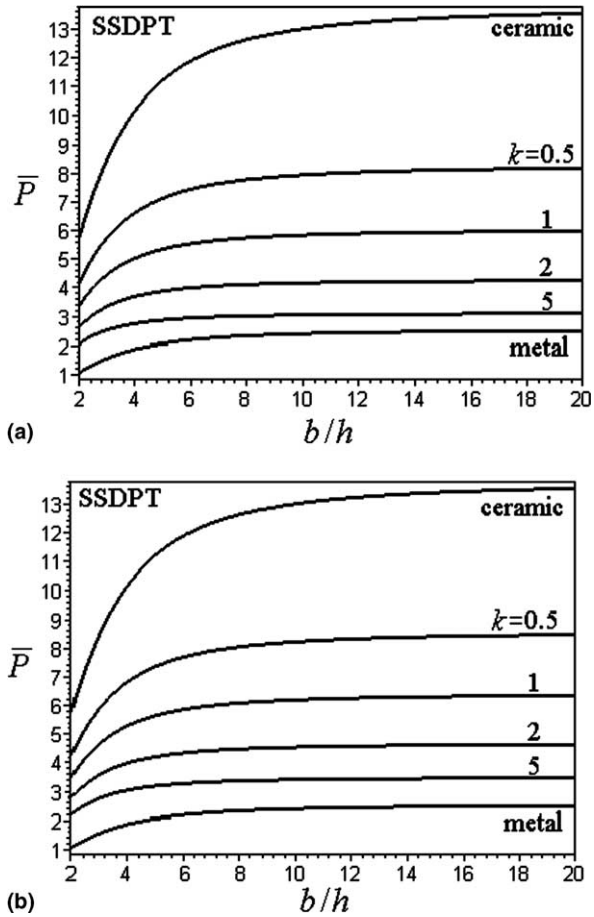

Fig. 6. Biaxial buckling load $(\overline{P})$ as a function of side-to-thickness ratio (b/h) of symmetric and non-symmetric FGM sandwich plates for various values of k $(\gamma = 1)$. (a) The (2-1-2) FGM sandwich plate and (b) the (2-1-1) FGM sandwich plate.

metal plates. It is seen that the results increase smoothly as the amount of ceramic in the sandwich plate increases.

5. Concluding remarks

The critical buckling loads and the vibration frequencies of the sinusoidal plate theory, the third-order plate theory, the first-order plate theory and the classical thin plate theory for functionally graded plates have been established. The present sinusoidal theory contains the same dependent unknowns as first- and third-order shear deformation theories, but accounts according to a cosine-law distribution of the transverse shear strains through the thickness of the plate. Some available analogies between single-layer homogeneous plates, symmetric and non-symmetric functionally graded sandwich plates are special cases of the present results. As the ceramic constituent increases in the functionally graded sandwich plate, i.e., the volume fraction exponent decreases, all of the critical buckling loads and the vibration frequencies increase. In particular, the results of a homogeneous ceramic plate and a homogeneous metal plate are, respectively, the upper and lower bounds of those of the functionally graded sandwich plate.

Appendix A

The elements of the symmetric matrix $[R]$ are given according to the different theories by:

SSDPT and TSDPT:

$$R^{11} = R^{22} = -I^{11}, \quad R^{33} = -I^{11} - I^{22}(\lambda^2 + \mu^2), \quad R^{44} = R^{55} = -I^{33}, \quad R^{13} = \lambda I^{12},$$
$$R^{23} = \mu I^{12}, \quad R^{14} = R^{25} = -I^{13}, \quad R^{34} = \lambda I^{23}, \quad R^{35} = \mu I^{23}, \quad R^{12} = R^{15} = R^{24} = R^{45} = 0.$$

FSDPT:

$$R^{11} = R^{22} = -I^{11}, \quad R^{33} = -I^{11} - I^{22}(\lambda^2 + \mu^2), \quad R^{44} = R^{55} = -I^{22}, \quad R^{13} = \lambda I^{12},$$
$$R^{23} = \mu I^{12}, \quad R^{14} = R^{25} = -I^{12}, \quad R^{34} = \lambda I^{22}, \quad R^{35} = \mu I^{22}, \quad R^{12} = R^{15} = R^{24} = R^{45} = 0.$$

CLPT:

$$R^{11} = R^{22} = -I^{11}, \quad R^{12} = 0, \quad R^{13} = \lambda I^{12}, \quad R^{23} = \mu I^{12}, \quad R^{33} = -I^{11} - I^{22}(\lambda^2 + \mu^2).$$

References

Birman, V., 1995. Buckling of functionally graded hybrid composite plates. In: Proceeding of the 10th Conference on Engineering Mechanics 2, pp. 1199–1202.

Cheng, Z.Q., Batra, R.C., 2000a. Deflection relationships between the homogeneous Kirchhoff plate theory and different functionally graded plate theories. Archives of Mechanics 52, 143–158.

Cheng, Z.Q., Batra, R.C., 2000b. Three-dimensional thermoelastic deformations of a functionally graded elliptic plate. Composites Part B 31, 97–106.

Cheng, Z.Q., Batra, R.C., 2000c. Exact correspondence between eigenvalues of membranes and functionally graded simply supported polygonal plates. Journal of Sound and Vibration 229, 879–895.

Fukui, Y., Yamanaka, N., 1992. Elastic analysis for thick-walled tubes of functionally graded material subjected to internal pressure. International Journal of Japan Society of Mechanical Engineers, Series A 35, 379–385.

FGM Forum, 1991. Survey for application of FGM, Tokyo, Japan, Soc. Non Tradition Tech.

Hasselman, D.P.H., Youngblood, G.E., 1978. Enhanced thermal stress resistance of structural ceramics with thermal conductivity gradient. Journal of the American Ceramic Society 61, 49–53.

Javaheri, R., Eslami, M.R., 2002a. Thermoelastic buckling of rectangular plates made of functionally graded materials. AIAA Journal 40, 162–169.

Javaheri, R., Eslami, M.R., 2002b. Buckling of functionally graded plates under in-plane compressive loading. ZAMM 82, 277–283.

Javaheri, R., Eslami, M.R., 2002c. Thermal buckling of functionally graded plates based on higher order theory. Journal of Thermal Stresses 25, 603–625.

Koizumi, M., 1993. The concept of FGM. Ceramic Trans., Functionally Gradient Materials 34, 3–10.

Leissa, A.W., 1973. The free vibration of rectangular plates. Journal of Sound and Vibration 31, 257–293.

Librescu, L., Khdeir, A.A., Reddy, J.N., 1990. Further results concerning the dynamic response of shear deformable elastic orthotropic plates. ZAMM 70, 23–33.

Loy, C.T., Lam, K.Y., Reddy, J.N., 1999. Vibration of functionally graded cylindrical shells. International Journal of Mechanical Sciences 41, 309–324.

Malik, M., Bert, C.W., 1998. Three-dimensional elasticity solutions for free vibrations of rectangular plates by the differential quadrature method. International Journal of Solids and Structures 35, 299–318.

Najafizadeh, M.M., Eslami, M.R., 2002a. First-order-theory-based thermoelastic stability of functionally graded material circular plates. AIAA Journal 40, 1444–1450.

Najafizadeh, M.M., Eslami, M.R., 2002b. Buckling analysis of circular plates of functionally graded materials under uniform radial compression. International Journal of Mechanical Sciences 44, 2479–2493.

Ng, T.Y., Lam, Y.K., Liew, K.M., Reddy, J.N., 2001. Dynamic stability of functionally graded cylindrical shell under periodic axial loading. International Journal of Solids and Structures 38, 1295–1300.

Praveen, G.N., Reddy, J.N., 1998. Nonlinear transient thermoelastic analysis of functionally graded ceramic–metal plates. International Journal of Solids and Structures 35, 4457–4476.

Reddy, J.N., 1984. A refined nonlinear theory of plates with transverse shear deformation. International Journal of Solids and Structures 20, 881–896.

Reddy, J.N., 2000. Analysis of functionally graded plates. International Journal for Numerical Methods in Engineering 47, 663–684.

Reddy, J.N., Chin, C.D., 1998. Thermomechanical analysis of functionally graded cylinders and plates. Journal of Thermal Stresses 21, 593–626.

Vel, S.S., Batra, R.C., 2002. Exact solution for thermoelastic deformations of functionally graded thick rectangular plates. AIAA Journal 40, 1421–1433.

Yamanouchi, M., Koizumi, M., Hirai, T., Shiota, I. (Eds.), 1990. In: Proceedings of the First International Symposium on Functionally Gradient Materials, Sendai, Japan.

Zenkour, A.M., 2004a. Thermal effects on the bending response of fiber-reinforced viscoelastic composite plates using a sinusoidal shear deformation theory. Acta Mechanica 171, 171–187.

Zenkour, A.M., 2004b. Analytical solution for bending of cross-ply laminated plates under thermo-mechanical loading. Composite Structures 65, 367–379.

Zenkour, A.M., 2004c. Buckling of fiber-reinforced viscoelastic composite plates using various plate theories. Journal of Engineering Mathematics 50, 75–93.

Zenkour, A.M., 2005a. A comprehensive analysis of functionally graded sandwich plates: Part 1—Deflection and stresses. International Journal of Solids and Structures, in press, doi:10.1016/j.ijsolstr.2005.02.015.

Zenkour, A.M., 2005b. Generalized shear deformation theory for bending analysis of functionally graded plates. Applied Mathematical Modelling, in press.